Research in Astronomy and Astrophysics, 23:105002 (8pp), 2023 October https://doi.org/10.1088/1674-4527/acee4e

Narrowband EUV Sc/Si Multilayer for the Solar Upper Transition Region Imager at 46.5 nm

Runze Qi[1,2], Jiali Wu[1,2], Jun Yu[1,2], Chunling He[1,2], Li Jiang[1,2], Yue Yu[1,2], Zhe Zhang[1,2], Qiushi Huang[1,2], Zhong Zhang[1,2], and Zhanshan Wang[1,2]

[1] Key Laboratory of Advanced Micro-structured Materials, Ministry of Education, Tongji University, Shanghai 200092, China; wangzs@tongji.edu.cn
[2] Institute of Precision Optical Engineering, School of Physics Science and Engineering, Tongji University, Shanghai 200092, China
Received 2023 April 13; revised 2023 June 25; accepted 2023 June 28; published 2023 September 19

Abstract

The transition region is the key region between the lower solar atmosphere and the corona, which has been limitedly understood by human beings. Therefore, the Solar Upper Transition Region Imager (SUTRI) was proposed by Chinese scientists and launched in 2022 July. Right now, the first imaging observation of the upper transition region around 46.5 nm has been carried out by SUTRI. To ensure the spectral and temporal resolution of the SUTRI telescope, we have developed a narrowband Sc/Si multilayer. Based on the extreme ultraviolet (EUV) reflectivity measurements, the multilayer structure has been modified for ensuring the peak position of reflectivity was at 46.5 nm. Finally, the narrowband Sc/Si multilayer was successfully deposited on the hyperboloid primary mirror and secondary mirrors. The deviation of multilayer thickness uniformity was below than 1%, and the average EUV reflectivity at 46.1 nm was 27.8% with a near-normal incident angle of 5°. The calculated bandwidth of the reflectivity curve after primary and secondary mirrors was 2.82 nm, which could ensure the requirements of spectral resolution and reflectivity of SUTRI telescope to achieve its scientific goals.

Key words: Astronomical Instrumentation – Methods and Techniques – instrumentation: high angular resolution – Sun: UV radiation

1. Introduction

The Sun is the ultimate source of matter and energy on Earth, and there are still many unknowns about it, such as how the million-degree heat is generated in corona? What is the origin of the solar winds? What is the mechanism that causes solar eruptions (Innes et al. 1997; Hassler et al. 1999; Tu et al. 2005). All of these problems are important to contemporary astronomy. The solar atmosphere is composed of a photosphere, chromosphere, transition region (TR) and corona. The TR is the important region connecting the lower solar atmosphere and the corona. It is a dynamic and highly nonuniform regime with the temperature from 0.02 MK to 0.8 MK and magnetic field changing sharply. The observations have proven that the TR is essential for the matter and energy transport in the quiet solar atmosphere and solar eruptions (Peter et al. 2014; Tian 2014). To explore the activity in the TR, a specific telescope has been proposed by Chinese scientists. Based on a mission concept study and advanced research of space science missions, the Solar Upper Transition Region Imager (SUTRI) project had been proposed which was launched in 2022 July. The SUTRI focused on the strongest emission lines formed in temperature regime around 0.5 MK, which is the Ne VII line at 46.5 nm. The normal-incidence multilayers are coated on the primary and secondary mirrors to enhance the efficiency of the target Ne VII line at 46.5 nm and avoid the influence from other emission lines. To achieve the observation objective, the bandwidth ($\Delta\lambda$, the width of the band at half the height of the reflectance peak) after twice reflections should be less than 3 nm, and the single reflection efficiency should be higher than 22%.

Sc/Si multilayer is a promising combination and possesses high theoretical reflectivity and temporal stability at 46.5 nm. In 1998, (Uspenskii et al. 1998) prepared Sc/Si multilayers with different periods by magnetron sputtering and measured that the peak reflectance at 36.5 nm wavelength was 54% and the bandwidth was 5.5 nm. It is found that the diffusion of Sc and Si at the interface is the main reason for the decrease in reflectivity. Subsequently, researchers tried to introduce W, B_4C, ScN, CrB_2, and other barrier layers at the Sc/Si multilayer interface. Although the thermal stability was improved, the reflectivity was not significantly improved (Vinogradov et al. 2001; Gautier et al. 2005; Pershyn et al. 2011). The Sc/Cr/Si multilayer with $\Gamma_{Sc} = d_{Sc}/D = 0.4$ (Γ_{Sc} represents the thickness ratio to the d-spacing of the multilayer, d_{Sc} represents the thickness of Sc layer, and D represents the d-spacing of the multilayer, equal to the bilayer thickness) had a reflectance of 56.6% at the wavelength of 44.7 nm, which was the highest reflectivity until now, and its bandwidth was 4.8 nm (Yulin et al. 2004). In 2018, Pershyn et al. (Pershyn et al. 2018) prepared Sc/C/Si/C multilayers by magnetron sputtering and

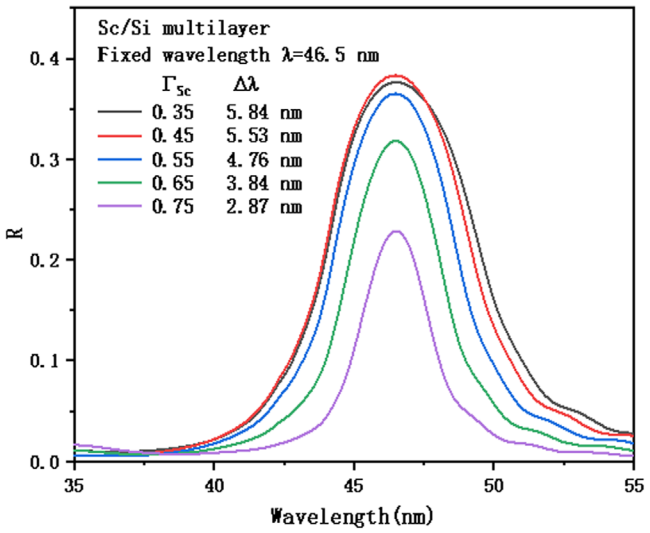

Figure 1. Theoretical reflectivity of the Sc/Si multilayers with different Γ_{Sc} values working at 46.5 nm.

studied the influence of barrier layers C with different thickness on the reflectance and interface structure of the multilayers. Carbon reacted with scandium and silicon to form an asymmetric interface. The compound of the Si-on-Sc interface was carbide, and the compound of the Sc-on-Si interface was silicon carbide. In 2020, Zhu et al. (Zhu et al. 2020) prepared Sc/B_4C/Si/B_4C multilayers and Sc/C/Si/C multilayers with different thickness barrier layers by magnetron sputtering. By introducing B_4C and C as barrier layers, the thermal stability of Sc/Si multilayers was improved, reaching 300° and 400° respectively, but the extreme ultraviolet reflectance was not mentioned.

As seen in previous work, most authors paid more attention to the highest reflectivity of the Sc/Si multilayer under a general thickness ratio of 0.4–0.5 and the improvement of the thermal stability, but the reflectance bandwidth of the Sc/Si multilayer was almost more than 4.5 nm, not met the narrow bandwidth requirement of the SUTRI telescope. SUTRI used the Ritchey-Chrétien (RC) optical design (Martínez-Galarce et al. 2013), in which the clear aperture diameter of the primary was 190 mm and that of the secondary mirror was 40 mm. To realize the thickness uniformity on large-size hyperboloid mirrors is also key to ensuring the spectral purity and efficiency of the whole optical system. This paper detailed presents the development of stable narrowband Sc/Si multilayer mirrors with high thickness uniformity in the SUTRI telescope.

2. Design

The SUTRI telescope is a high-spectral-imager which relies on multilayer mirrors to achieve monochromic imaging. However, there were many emission lines around the Ne VII line which might be the influence the purity of signal. For reflecting the Ne VII line and suppressing the surroundings (Del Zanna et al. 2001), the reflection bandwidth of two mirrors required less than 3 nm. Varying the layer thickness ratio between Sc layer thickness and the bilayer thickness was the common and efficient method to change the reflection bandwidth (Lim et al. 2001). The designed Sc/Si multilayer had 20 bilayers. Considering the interfacial diffusion and surface oxidation, the reflectivity curves of the Sc/Si multilayers with different Γ_{Sc} values were calculated by the IMD software (Windt 1998) and presented in Figure 1. With increasing Γ_{Sc} from 0.35 to 0.75, the reflectivity decreased from 37.6% to 22.8% and the corresponding bandwidth also decreased from 5.84 to 2.87 nm. It was noted that the bandwidth and reflectivity decreased simultaneously when increasing Γ_{Sc}. For the narrowband requirement and relatively high reflectivity, the *d*-spacing and Γ_{Sc} values of the Sc/Si multilayer had been determined to be 23.38 nm and 0.65, respectively. The incidence angles range from 1.8° to 4.8° across a clear aperture of 45–90 mm for the primary mirror and from 2.2° to 7.3° across a clear aperture of 17–38.5 mm for the secondary mirror. As shown in Figure 2(a), the theoretical efficiency of the Sc/Si multilayer after two reflections varied slightly as a function of the incidence angle. In addition, 0.5% of thickness deviation during the deposition process was taken into account in the reflectivity calculation, as shown in Figure 2(b). Despite the offset of the peak position caused by the thickness deviation, it was acceptable that the reflectivity at 46.5 nm exceeds 30% and the bandwidth is less than 3 nm.

3. Deposition and Measurements

3.1. Precisely Control of the Thickness Uniformity on a Large-size Hyperboloid Mirror

The multilayer thickness uniformity determines the monochromatic ability and optical efficiency of the whole optical system. The deviation of the multilayer thickness would cause an offset in the central peak position of the reflectivity curve, decreasing reflectivity at 46.5 nm. In the SUTRI telescope, the shape of the large-size primary mirror is hyperboloid and the clear aperture diameter of 190 mm, and main characteristics of the primary mirror are presented in Table 1. It demonstrated that the precise control of the thickness uniformity of a large-size hyperboloid mirror is the first problem to be solved during the deposition.

All Sc/Si multilayers on Si substrates and curved hyperboloid substrates were deposited by direct-current (DC) magnetron sputtering system having a high-vacuum chamber with a diameter of 1.20 m and height of 0.65 m (Zhang et al. 2019). As shown in Figure 3, the layer thickness depends on the speed of multilayer sample movement over the sputtering target, and the substrate rotated around the sample holder's axis of symmetry at a speed of 400 rpm to achieve good radial

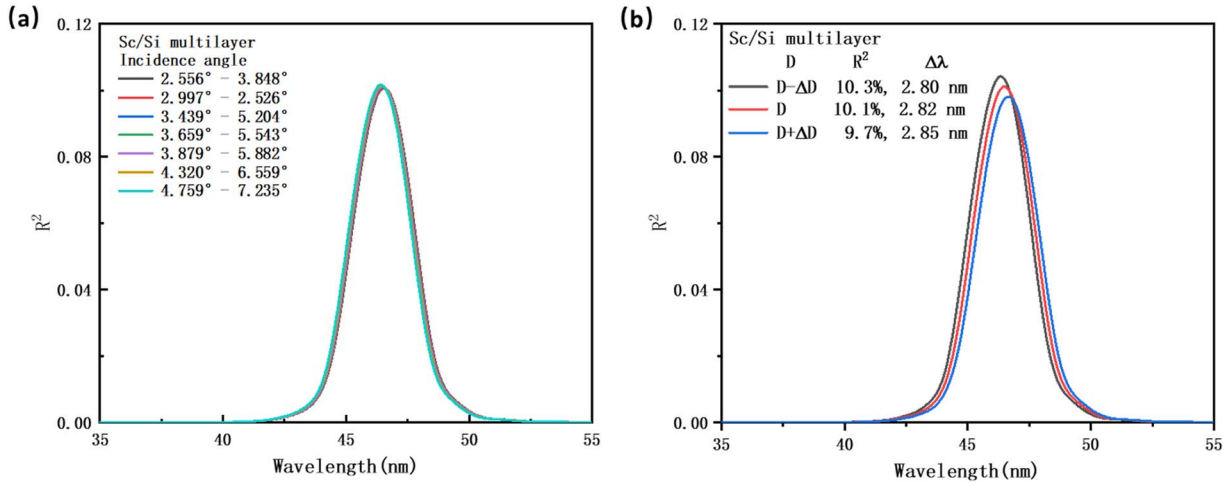

Figure 2. (a) Theoretical efficiency of Sc/Si multilayers after two reflections as a function of incidence angle; (b) Theoretical efficiency of Sc/Si multilayers with thickness deviation.

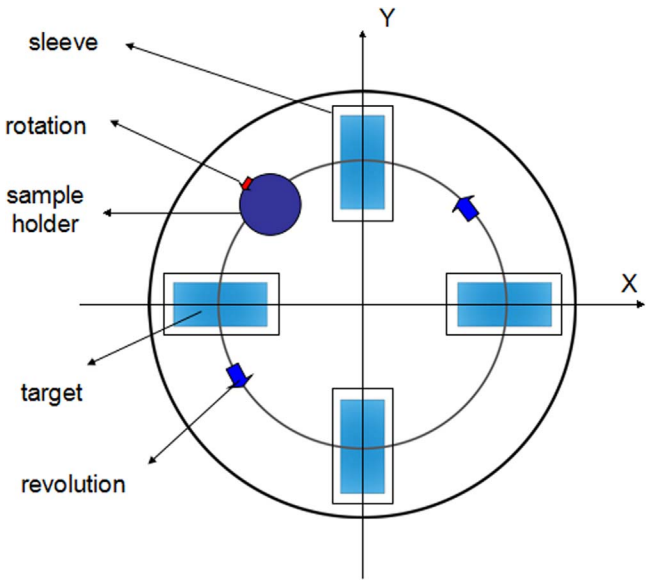

Figure 3. Schematic of the DC magnetron sputtering system.

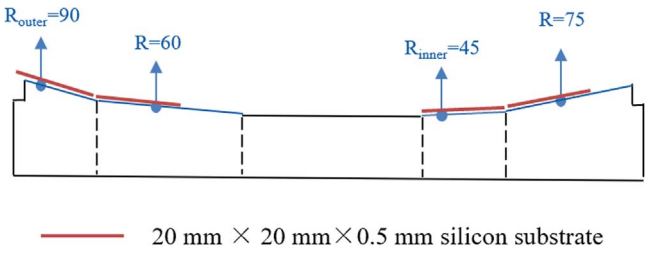

Figure 4. Schematic illustration of the mirror substitute design.

Table 1
Main Characteristics of the Primary Mirror in the SUTRI Telescope

Parameters	Value
Radius of curvature/mm	1164
Conic value	1.404 54
External diameter/mm	95
Outer effective aperture R_{outer}/mm	90
Inner effective aperture R_{inner}/mm	45
Incidence angle/degrees	1.8–4.8

uniformity (Yu et al. 2015; Oliver 2017). In the deposition process, the base vacuum was less than 10^{-4} Pa, high-purity argon (99.999%) was used as the sputtering gas and the gas pressure was 1.1 mTorr. The sputtering power of Sc and Si targets was 200 W and 300 W, respectively. The successive layers were deposited above a target at a distance of 11.5 cm.

During the deposition, the multilayer thickness on the primary mirror could not be directly measured, a mirror substitute was reconstructed on the same curved surface and prepared to estimate the values of selected points on the coating surface under rotating conditions. The multilayer thickness uniformity control at different radius positions on the mirror substitute was achieved by adjusting the rate curve of revolution. In Figure 4, the Sc/Si multilayer thickness distribution was selected as four points between the center of the primary mirror and its boundary, and the center position at $R_{inner} = 45$ mm was taken as the reference point. The tangent line was used to create a cross-sectional line.

The results of the Grazing incidence X-ray reflectometry (GIXR) measurements are shown in Figure 5(a) by the point line after normalized reflection intensity. The curves were

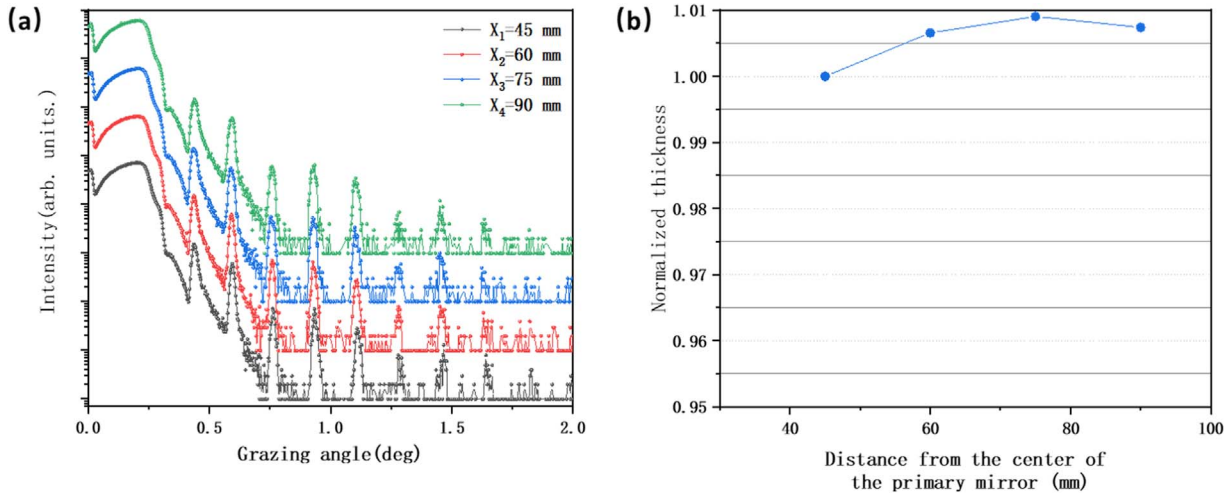

Figure 5. (a) GIXR measurements of the multilayer deposited on different positions; (b) Normalized thickness profiles as function of distance from the center of the primary mirror.

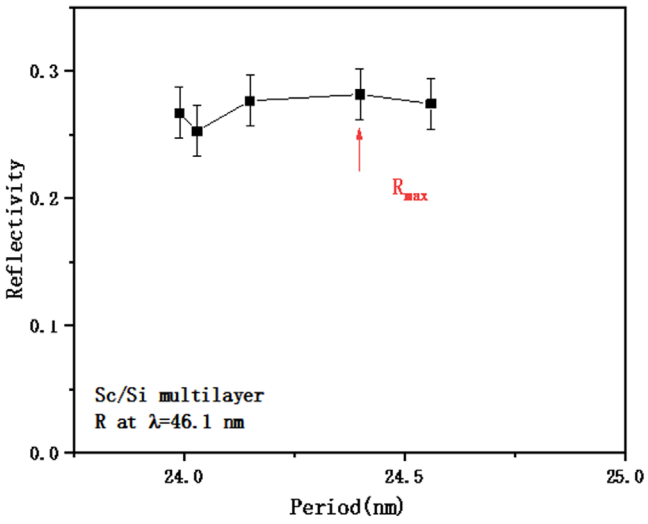

Figure 6. The reflectivity of the Sc/Si multilayers with different *d*-spacings at 46.1 nm.

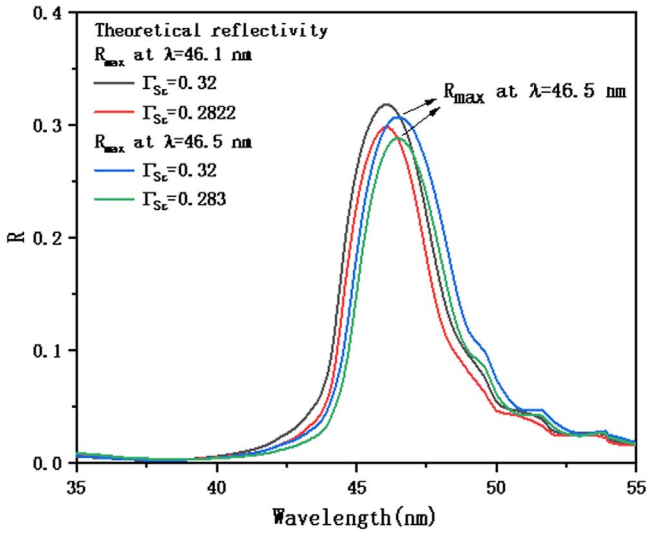

Figure 7. The reflectivity of the Sc/Si multilayers with different *d*-spacings at 46.1 nm and 46.5 nm.

shifted vertically for clarity. It was found that in the GIXR reflectivity curves, the peak position and peak width of Bragg peaks of the multilayer at each position were consistent, indicating good film thickness uniformity and excellent film forming quality. Bede reference software was used to fit the reflectivity curve to obtain the individual layer thickness and roughness. The corresponding measured thickness along the radial axis is normalized and presented in Figure 5(b). The normalized thickness for each point was obtained by dividing the bilayer thickness at that point by the bilayer thickness at the reference point. The position of the silicon substrate which was the closest to the center of the mirror was taken as the reference point. The thickness error of the multilayer at different positions was lower than 1%.

3.2. Multilayer Structure Correction Guided by Laboratory-based EUV Reflectometer

Accurate optical constants could guide the design of multilayer structures and the calculation of theoretical reflectivity. But there are many aspects which lead to a mismatch between the theoretical and measured reflectivity, such as the imperfections at the interfaces, oxidation/contamination, the crystalline state of the layer, and inaccurate optical constants of

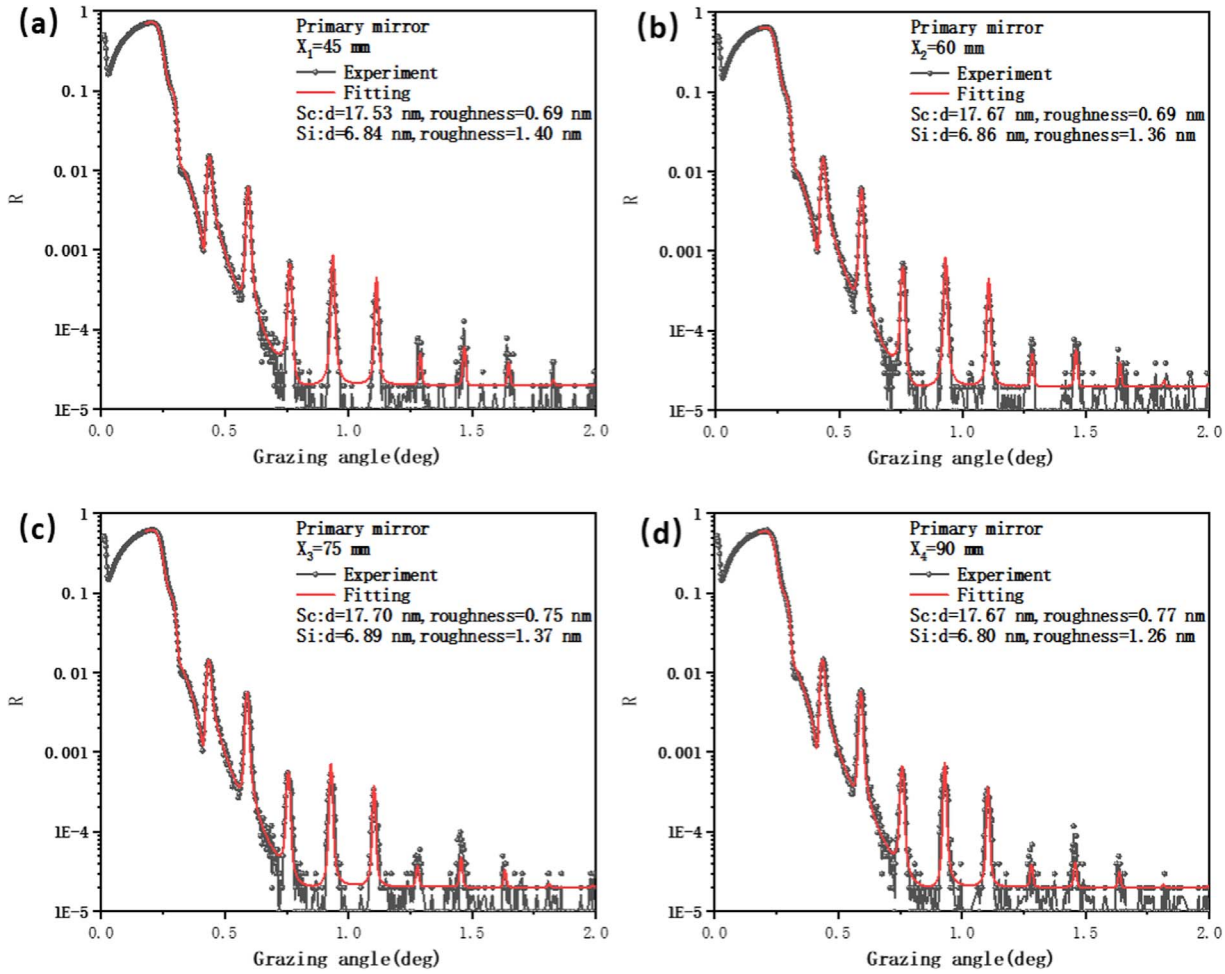

Figure 8. The measured results and fitted GIXR curves for each point of the multilayers deposited on the primary mirror substitute.

the materials at >35 nm (Polkovnikov et al. 2019). Thus, it was important to correct Sc/Si multilayer structure for operating 46.5 nm. A laboratory-based EUV reflectometer with an operational wavelength range of 30–200 nm was developed at the Institute of Precision Optical Engineering (IPOE) for characterizing the reflectivity of thin films. The measurement accuracy of the system is better than 0.5% and the repeatability of 2% (Yu et al. 2022). A radio-frequency-produced gas-discharge light source is applied to generate characteristic lines. The high brightness output can be achieved by the mixing of multiple gases. High purity Ne gas discharge as the light source can obtain a strong characteristic peak at 46.1 nm to meet the test requirements. The reflectivity test of the reflectometer guides the correction of the multilayer structure, ensuring the actual preparation of the multilayer.

The reflectivity of Sc/Si multilayers with the same $\Gamma_{Sc} = 0.32$ and different d-spacing were tested at a near-normal incidence angle, and the results are shown in Figure 6. When the d-spacing of Sc/Si multilayer was 24.40 nm, the reflectivity reached a maximum of $28.2\% \pm 2\%$ at 46.1 nm. Based on this structure, the Sc/Si multilayer with the central wavelength of 46.5 nm was calculated, as shown in Figure 7, and the Sc thickness ratio was further optimized to achieve the reflection bandwidth after two reflections less than 3 nm. It determined that the Sc/Si multilayer with d-spacing of 24.55 nm and $\Gamma_{Sc} = 0.283$ would work at the central wavelength of 46.5 nm and have relatively high reflectivity.

3.3. Results of the Primary and Secondary Mirrors

According to the corrected structural parameters, the Sc/Si multilayers were deposited on the mirror substitutes and the final mirrors under the same deposition parameters. The measured results and fitted GIXR curves for each point of the multilayers were shown in Figures 8 and 9, corresponding to test points on the primary and secondary mirror substitutes. The multilayer thickness distribution on both mirror substitutes was presented in Figure 10. The thickness uniformity deviation

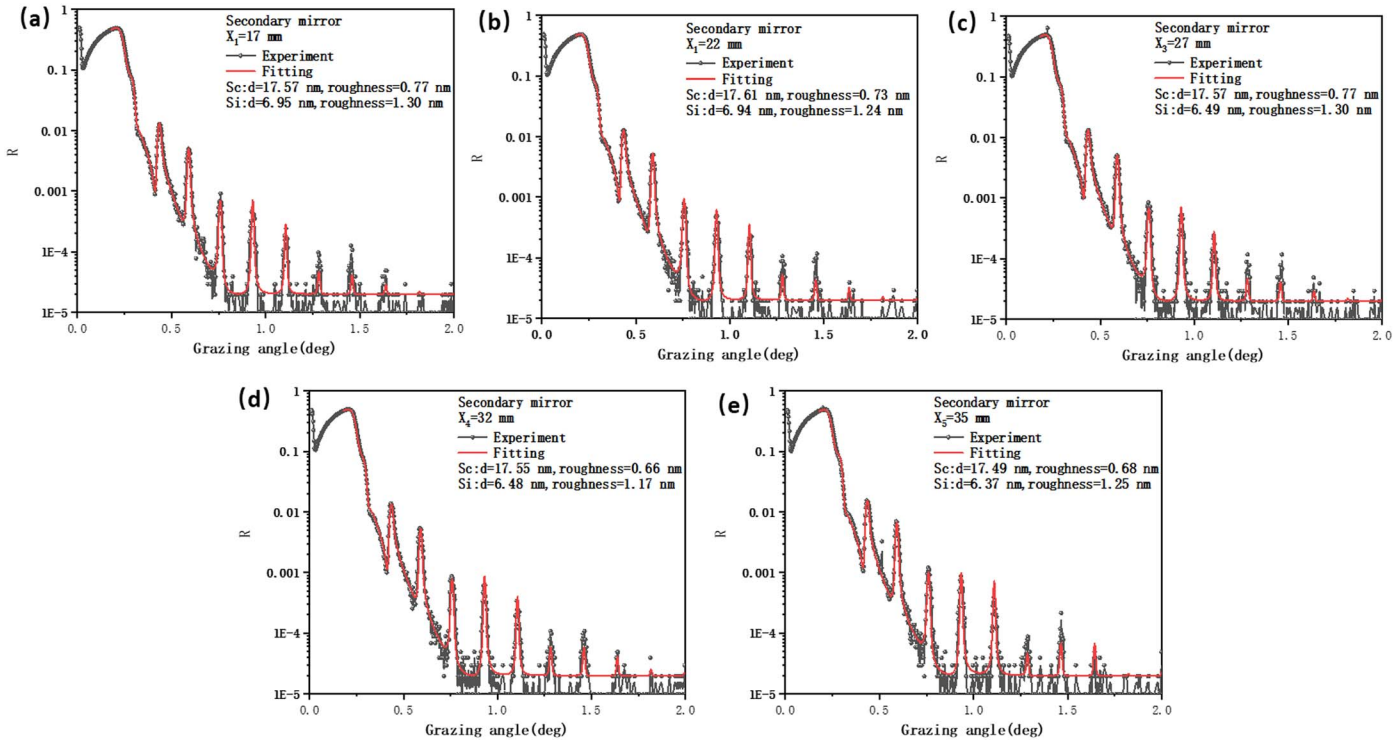

Figure 9. The measured results and fitted GIXR curves for each point of the multilayers deposited on the secondary mirror substitute.

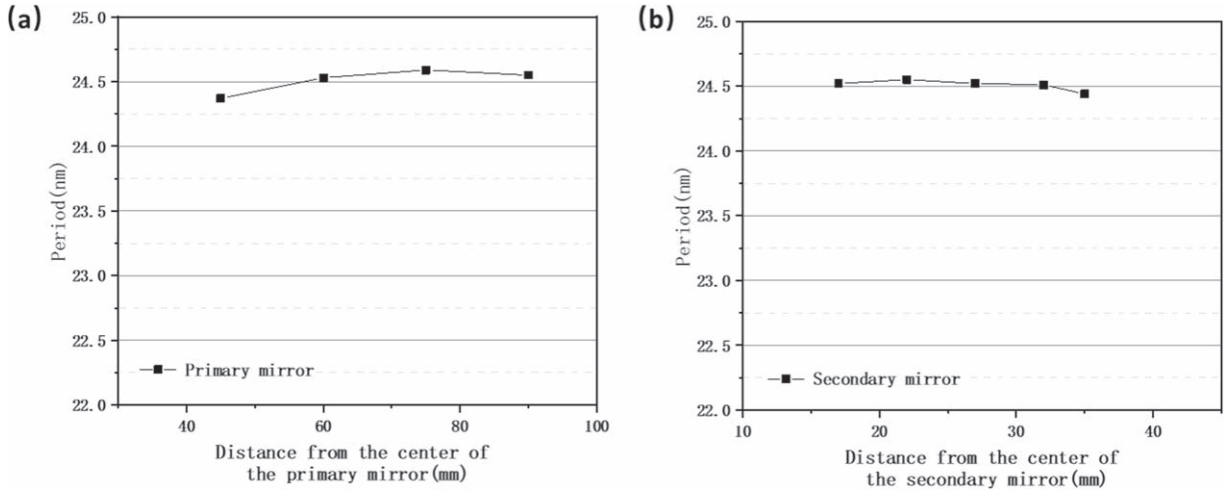

Figure 10. Multilayer *d*-spacing values as functions of the distance for (a) the primary mirror and (b) the secondary mirror.

of the multilayers deposited on the primary mirror substitute was less than 0.2 nm, and that of the multilayers deposited on the secondary mirror substitute was less than 0.1 nm. It demonstrated that the multilayer thickness uniformity control met the application requirement. Meanwhile, the central peak position under actual preparation was estimated to be 46.5 nm, reflectivity of 24.6%, and a bandwidth of 3.7 nm. After twice reflections, the efficiency was 6.0% with a bandwidth of 2.8 nm as shown in Figure 11. Finally, the reflectivity of the primary mirror at $X_1 = 45$ mm (the distance between the first measured position and the center of the mirror) and the secondary mirror at $X_1 = 17$ mm was tested by a laboratory-based EUV reflectometer and obtained 28.0% and 27.7%, and the average reflectivity was 27.8%. The objectives of the primary mirror

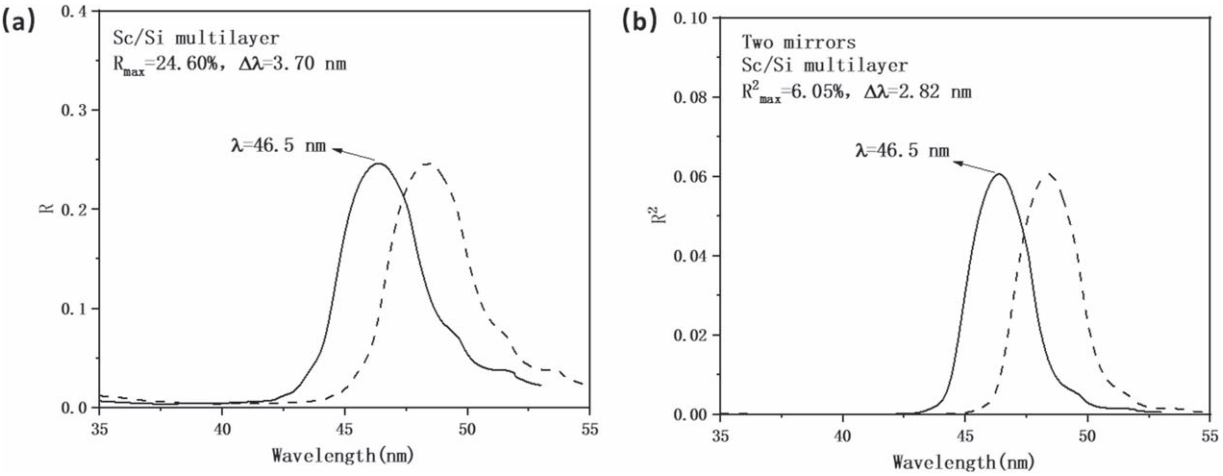

Figure 11. (a) Theoretical EUV reflectivity of the Sc/Si multilayer after one reflection; (b) Theoretical efficiency of the Sc/Si multilayer after two reflections.

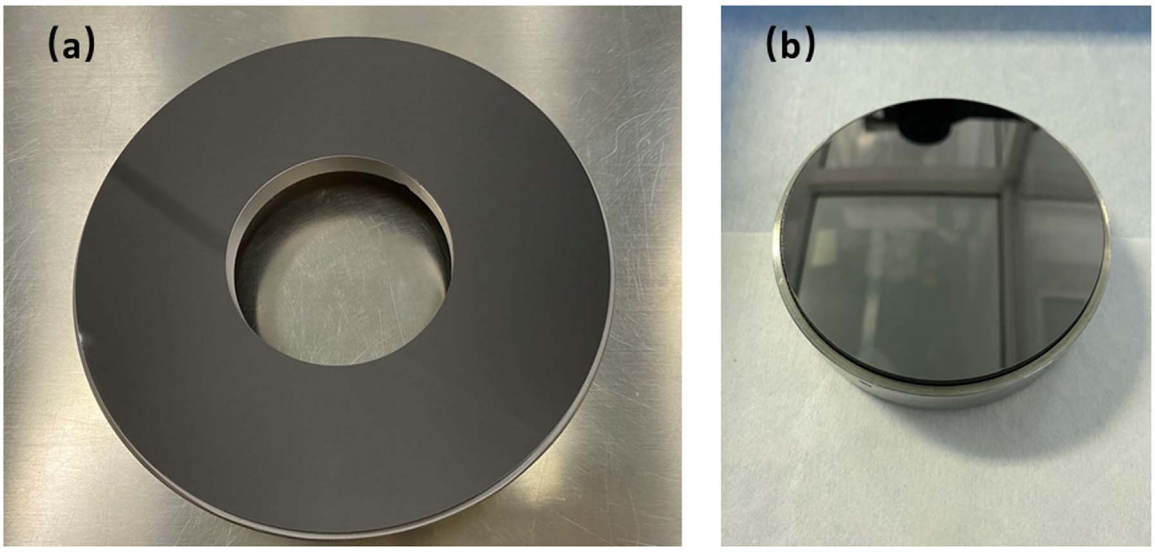

Figure 12. The primary and the secondary mirrors.

and the secondary mirror coated with Sc/Si multilayer were displayed in Figure 12.

4. Conclusion

Aiming for the dynamic imaging observation of the Ne VII line (0.5 MK) in the upper transition region, we present experimental results on the development and testing of stable narrowband Sc/Si multilayers operating at 46.5 nm. To realize the bandwidth requirements, the Sc/Si multilayer mirror with a *d*-spacing of 24.55 nm and $\Gamma_{Sc} = 0.283$ was prepared on a 190 mm diameter primary mirror by DC magnetron sputtering. GIXR tests at different positions on the primary mirror showed a 1% deviation of thickness uniformity of Sc/Si multilayers on a large hyperboloid mirror with a diameter of 190 mm. The EUV reflectometer independently guided the correction of the multilayer structure, and finally realized the measured average reflectivity of the Sc/Si multilayer was 27.8% at the 46.1 nm wavelength at the incidence angle of 5°. This work ensured the development of the SUTRI and also reserved core technology for the Chinese Space exploration project.

Acknowledgments

This work was funded by the National Natural Science Foundation of China (NSFC) under Nos. 12003016, 12204353 and 62105244.

References

Del Zanna, G., Bromage, B. J. I., Landi, E., et al. 2001, A&A, 379, 708
Gautier, J., Delmotte, F., Roulliay, M., et al. 2005, Proc. SPIE, 5963, 59630X
Hassler, D. M., Dammasch, I. E., Lemaire, P., et al. 1999, Science, 283, 810
Innes, D. E., Inhester, B., Axford, W. I., et al. 1997, Nature, 386, 811
Lim, Y. C., Westerwalbesloh, T., Aschentrup, A., et al. 2001, ApPhA, 1, 121
Martínez-Galarce, D., Soufli, R., Windt, D. L., et al. 2013, OptEn, 52, 095102
Oliver, J. B. 2017, ApOpt, 56, 5121
Pershyn, Y. P., Zubarev, E. N., Kondratenko, V. V., et al. 2011, ApPhA, 103, 1021
Pershyn, Y. P., Zubarev, E. N., Kondratenko, V. V., et al. 2018, Funct. Mater., 25, 505
Peter, H., Tian, H., Curdt, W., et al. 2014, Sci., 346, 1255726
Polkovnikov, V. N., Chkhalo, N. I., Meltchakov, E., et al. 2019, TePhL, 45, 85
Tian, H. 2014, RAA, 17, 110
Tu, C., Zhou, C., Marsch, E., et al. 2005, Science, 308, 519
Uspenskii, Yu. A., Levashov, V. E., Vinogradov, A. V., et al. 1998, Nm. OptL, 23, 771
Vinogradov, A. V., Pershin, Y. P., Zubaryev, E., et al. 2001, Proc. SPIE, 4505, 230
Windt, D. L. 1998, JCoPh, 12, 360
Yu, B., Jin, C., Yao, S., et al. 2015, OptL, 40, 3958
Yu, Y., Ye, Z., Jiang, L., et al. 2022, JATIS, 8, 017002
Yulin, S. A., Schaefers, F., Feigl, T., et al. 2004, Proc. SPIE, 5193, 155
Zhang, Z., Qi, R., Yao, Y., et al. 2019, Coatings, 9, 851
Zhu, J., Zhang, J., Jiang, H., et al. 2020, ACS Appl. Mater. Interfaces, 12, 25400